Highlights

FRACTAL MIXTURES FOR OPTIMAL HEAT DRAINING

Massimo Cefalo, Simone Creo, Maria Rosaria Lancia, Javier Rodríguez-Cuadrado

- We optimize the shape of Koch-mixture interfaces to drain heat in a bulk
- We propose a fractal dynamics which takes into account the heat fluxes.
- We use an optimal mesh algorithm for Koch interfaces to compute the temperature.
- Asymmetric Koch-mixture interfaces are suitable to drain heat when properly refined.
- The conductivity of the interface plays a significant role in the optimal shape.

FRACTAL MIXTURES FOR OPTIMAL HEAT DRAINING

Massimo Cefalo[a], Simone Creo[b], Maria Rosaria Lancia[b], Javier Rodríguez-Cuadrado[c,*]

[a] *Dipartimento di Ingegneria Informatica, Automatica e Gestionale, Sapienza Università di Roma, Rome, Italy*
[b] *Dipartimento di Scienze di Base e Applicate per l'Ingegneria, Sapienza Università di Roma, Rome, Italy*
[c] *Departamento de Matemática Aplicada a la Ingeniería Industrial, Universidad Politécnica de Madrid, Ronda de Valencia 3, Madrid, 28012, Spain*

Abstract

The aim of this paper is to optimize the shape of a highly conductive interface in order to drain the maximum amount of heat. Given the ubiquity of irregular interfaces in heat transmission processes, we model such interfaces by Koch-mixture fractal layers. We propose a dynamics that iteratively refines these mixtures in order to maximize the temperature reduction in the bulk. We obtain that asymmetric Koch-mixtures drain heat effectively when properly refined. In addition, we show that the conductivity of the interface plays a significant role in the refinement of the optimal shape.

Keywords: Asymmetric fractal mixtures, Optimal shape, Heat flow, Highly conductive layers

1. Introduction

Irregular layers and media are involved in many physical phenomena, such as diffusion processes in physical membranes, current flow across rough electrodes in electrochemistry and diffusion of sprays in the lungs (see e.g. [1, 2]). In particular, the role of surface roughness has a deep impact in industrial applications, e.g. in coating technology and the design of microelectro-mechanical systems (MEMS) [3, 4, 5, 6, 7]. These phenomena are typically described by parabolic boundary value problems (BVPs) involving a transmission condition of order zero, one or two where the irregular media is modeled by fractal-type boundaries and/or interfaces. Thus, the numerical approximation of the corresponding boundary value problems is crucial to predict or confirm the experimental evidence.

The first results on the numerical approximation of BVPs in domains with fractal-type boundaries and/or interfaces go back to the last 20 years [8, 9, 10, 11, 12, 13], where the main focus was on heat transfer problems across a given highly conductive pre-fractal boundary

*Corresponding author

Email addresses: cefalo@dis.uniroma1.it (Massimo Cefalo), simone.creo@uniroma1.it (Simone Creo), mariarosaria.lancia@uniroma1.it (Maria Rosaria Lancia), javier.rodriguez.cuadrado@upm.es (Javier Rodríguez-Cuadrado)

and/or interface (i.e. second order transmission conditions). From the numerical simulations performed in such papers, it results that fractal-type interfaces are capable of draining heat from the bulk more efficiently than a flat interface, as described in [10]. This fact can be usefully exploited from the point of view of applications.

In many industrial applications it is crucial to know which is the "optimal" interface to drain heat from heat sources. The mathematical model must be a control problem in which the dynamics of a pre-fractal barrier evolves automatically. Actually, the dynamics should be driven by the "feedback" of thermal flows, thus taking into account that the thermal sources located in the bulk are time dependent. The goal of the control system is to drain heat in an optimal way from the thermal sources.

The problem could be formalized as follows: given a bulk (with an internal interface/layer) where some heat sources are located, which is the optimal shape of the layer to drain the maximum amount of heat from the heat sources in a given time? Answering this question is the main goal of this paper and it first requires linking the concept of "draining heat" to a physical magnitude. For this reason, we assume that draining heat is equivalent to reducing the maximum temperature in the bulk. The mathematical problem that we aim to address in this paper is to obtain the optimal shape K^* of an interface, in a set $\mathscr{K}$ of possible pre-fractal sets that divides a bulk domain Ω in two subdomains Ω_1 and Ω_2 and minimizes the maximum temperature in the subdomain where the heat sources are supposed to be located.

This mathematical problem is denoted by $(\mathscr{P})$ and is formalized as

$$(\mathscr{P}) \qquad \min_{K\in\mathscr{K}} \max_{P\in\Omega} u_K(T,P),$$

where, for every given $K \in \mathscr{K}$, u_K is the solution of the second order transmission problem $(\overline{\mathscr{P}})$ formally stated as

$$(\overline{\mathscr{P}}) \begin{cases} \dfrac{\partial u(t,P)}{\partial t} - \Delta u(t,P) = f(P) & \text{in } [0,T]\times\Omega, \\ -\lambda \Delta_K u(t,P) = \left[\dfrac{\partial u(t,P)}{\partial \nu}\right] & \text{on } [0,T]\times K, \\ u(t,P) = 0 & \text{on } [0,T]\times\partial\Omega, \\ u(0,P) = 0 & \text{on } \overline{\Omega}, \end{cases}$$

where T is the time in which the stationary state is reached, Ω is a given bounded open subset of $\mathbb{R}^2$, K is a pre-fractal curve, Δ_K is the piecewise tangential Laplacian on K, λ is the layer conductivity, $\left[\frac{\partial u(t,P)}{\partial \nu}\right]$ is the jump of the normal derivative across K, ν is the outward unit normal vector and f is a given function in a suitable functional space.

Actually, to solve our problem $(\mathscr{P})$ is a complex task. To solve it, firstly, we assume that the heat sources are time independent and, secondly, we approach the solution iteratively. In particular, we propose a dynamics which makes the layer grow in each iteration according to thermal flows and other key physical magnitudes.

It is crucial to choose the set $\mathscr{K}$ in an efficient way both from the numerical and industrial application point of view. In this regard, we choose as set of possible layer configurations the set of Koch-type fractal mixtures. Our results show that asymmetric Koch mixtures, which are possible through a dynamics that makes the different parts of the layer grow independently, efficiently meet our aims.

The paper is organized as follows. In Section 2, we describe the geometry of the pre-fractal layers $K \in \mathscr{K}$. In Section 3, we show that for every given $K \in \mathscr{K}$, the problem $(\overline{\mathscr{P}})$ admits a unique "weak" solution. In Section 4, we study the numerical approximation of $(\overline{\mathscr{P}})$ by mixed methods (FEM in space and FD in time). In Section 5, we investigate problem $(\mathscr{P})$ by iteratively solving a sequence of simpler optimization problems $\{(\mathscr{P}_n)\}$, driven by a heuristic method which relies on the choice of a suitable "dynamics" which governs the growth of the interface. In Section 6, we present the results of the numerical simulations. Finally, in Section 7, we draw the conclusions and discuss the possibility to extend this work to the study of a control problem.

2. Preliminaries

2.1. The geometry

Fractal mixtures are constructed by employing the general iterated map system (see [14] and [15]).

Let $\mathscr{A}$ be a finite set of numbers greater than 1. For $\alpha \in \mathscr{A}$, let

$$\psi^{(\alpha)} = \left\{ \psi_1^{(\alpha)}, \dots, \psi_{N_\alpha}^{(\alpha)} \right\} \tag{2.1}$$

be a family of N_α contraction maps in $\mathbb{R}^2$ with contraction factor α^{-1}. Denote with $\Psi^{(\alpha)}$ the mapping in $\mathbb{R}^2$ defined by

$$\Psi^{(\alpha)}(E) = \bigcup_{i=1}^{N_\alpha} \psi_i^{(\alpha)}(E), \quad E \subset \mathbb{R}^2. \tag{2.2}$$

Let $\mathscr{A}^{\mathbb{N}}$ be the set of sequences $\xi = (\xi_1, \xi_2, \dots)$, with $\xi_i \in \mathscr{A}$. For $n \in \mathbb{N}$, let us define in $\mathbb{R}^2$ the following function:

$$\varphi_n^\xi = \Psi^{(\xi_1)} \circ \cdots \circ \Psi^{(\xi_n)} \tag{2.3}$$

where φ_0^ξ is the identity operator.

Let now Γ be a nonempty compact subset of $\mathbb{R}^2$ with $\Gamma \subset \Psi^{(\alpha)}(\Gamma)$, then the fractal mixture K^ξ associated with the sequence ξ is defined by

$$K^\xi = \overline{\left(\bigcup_{n=0}^{\infty} \varphi_n^\xi(\Gamma) \right)}. \tag{2.4}$$

For any fixed $\xi \in \mathscr{A}^{\mathbb{N}}$ and $n \in \mathbb{N}$, the set K^ξ is not strictly self-similar, but it does satisfy the property

$$K^\xi = \varphi_n^\xi \left(K^{\vartheta^n \xi} \right), \tag{2.5}$$

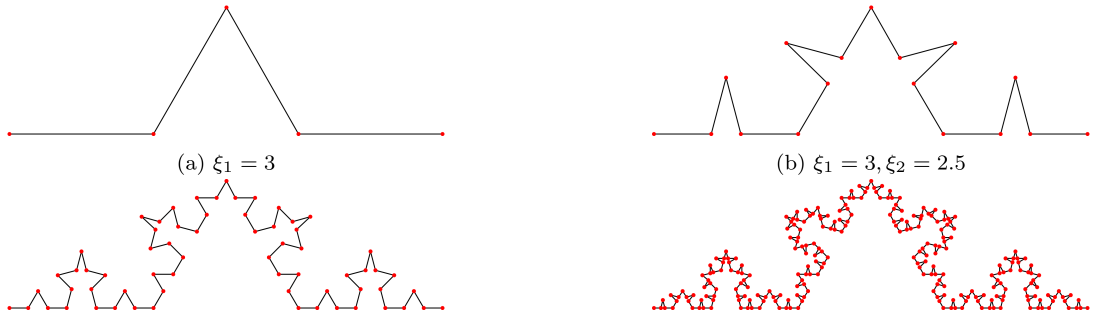

(a) $\xi_1 = 3$ (b) $\xi_1 = 3, \xi_2 = 2.5$

(c) $\xi_1 = 3, \xi_2 = 2.5, \xi_3 = 3$ (d) $\xi_1 = 3, \xi_2 = 2.5, \xi_3 = 3, \xi_4 = 2.5$

Figure 1: Pre-fractal Koch curve mixtures for variable length sequences of contraction factors.

where ϑ is the left shift operator on $\mathscr{A}^{\mathbb{N}}$ defined as $\vartheta\xi := (\xi_2, \xi_3, \dots)$ for $\xi = (\xi_1, \xi_2, \dots)$.

Given $\xi \in \mathscr{A}^{\mathbb{N}}$, we define

$$W_n^\xi = \otimes_{i=1}^n \{1, \dots, N_{\xi_i}\} \tag{2.6}$$

to be the set of all finite sequences of integers $w|n = (w_1, w_2, \dots, w_n)$ with $1 \leq w_i \leq N_{\xi_i}$ for $1 \leq i \leq n$. In addition, we set

$$\psi_{w|n}^\xi = \psi_{w_1}^{(\xi_1)} \circ \cdots \circ \psi_{w_n}^{(\xi_n)}. \tag{2.7}$$

Definition 2.1. *Let $A = (0,0)$, $B = (1,0)$ and $\Gamma = \{A, B\}$. Let $\mathscr{A}$ be a finite set of real numbers $\alpha \in (2,4)$. For a fixed sequence $\xi \in \mathscr{A}^{\mathbb{N}}$, the Koch curve mixture K^ξ defined in (2.4) is constructed by the families of contraction maps $\psi^{(\alpha)} = \left\{\psi_1^{(\alpha)}, \dots, \psi_4^{(\alpha)}\right\}$ in $\mathbb{C}$:*

$$\psi_1^{(\alpha)}(z) = \frac{z}{\alpha}, \qquad \psi_2^{(\alpha)}(z) = \frac{z}{\alpha}e^{i\theta} + \frac{1}{\alpha},$$
$$\psi_3^{(\alpha)}(z) = \frac{z}{\alpha}e^{-i\theta} + \frac{1}{2} + \frac{i\sin(\theta)}{\alpha}, \qquad \psi_4^{(\alpha)}(z) = \frac{z + \alpha - 1}{\alpha},$$

for $\alpha \in \mathscr{A}$, where $\theta = \cos^{-1}\left(\frac{\alpha}{2} - 1\right)$.

Let $\overline{\Gamma}$ be the unit segment connecting A and B. For fixed $\xi \in \mathscr{A}^{\mathbb{N}}$ and $n \in \mathbb{N}$, the n-th generation pre-fractal Koch curve mixture K_n^ξ is defined by

$$K_n^\xi := \varphi_n^\xi(\overline{\Gamma}). \tag{2.8}$$

For $\Gamma = \{A, B\}$ and $n \geq 0$, we define $V_n^\xi = \varphi_n^\xi(\Gamma)$. It can be seen that the following nested property of V_n^ξ holds:

$$V_0^\xi \subset V_1^\xi \subset \cdots \subset V_n^\xi. \tag{2.9}$$

In Figure 1, V_n^ξ and K_n^ξ are plotted in red and in black respectively.

Let $C^0(K^\xi)$ be the space of continuous functions on K^ξ and $C_0(K^\xi) := \{\phi \in C^0(K^\xi) :$

$\phi(A) = \phi(B) = 0\}$. Following [16], we know that there exists a unique Radon measure μ^ξ on K^ξ such that

$$\int_{K^\xi} \phi \, \mathrm{d}\mu^\xi = \sum_{w|n \in W_n^\xi} \left(N^\xi(n)\right)^{-1} \int_{K^{\vartheta^n \xi}} \phi \circ \psi^\xi_{w|n} \, \mathrm{d}\mu^{\vartheta^n \xi}, \tag{2.10}$$

for every $\phi \in C_0(K^\xi)$, where $N^\xi(n) = \Pi_{i=1}^n N_{\xi_i}$.

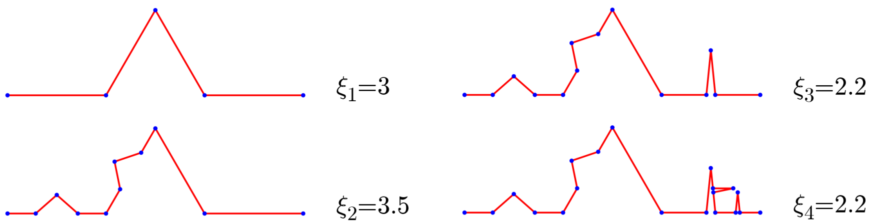

Figure 2: Asymmetric Kock-type mixtures for variable length sequences of contraction factors.

In the following, we will use asymmetric mixtures, which can be obtained from the previous procedure by choosing, at each iteration, a different contraction factor α for every contraction $\psi_i^{(\alpha)}$, for $i = 1, \ldots, 4$; see Figure 2.

2.2. Functional spaces

Let Ω be an open set of $\mathbb{R}^2$ with 2-dimensional Lebesgue measure $|\Omega|$. By $L^p(\Omega)$, for $p \geq 1$, we denote the Lebesgue space with respect to the two-dimensional Lebesgue measure $\mathscr{L}_2$, which will be left to the context whenever that does not create ambiguity. We denote by $C_0(\Omega)$ the space of continuous functions with compact support on Ω and by $C_0^\infty(\Omega)$ the smooth functions with compact support on Ω. We denote by $H^s(\Omega)$, $s \in \mathbb{R}^+$, the (fractional) Sobolev spaces with norm $\|\cdot\|_{H^s(\Omega)}$ and semi-norm $|\cdot|_{H^s(\Omega)}$ (see [17]), and by $H_0^s(\Omega)$ the closure of $C_0^\infty(\Omega)$ under the norm $\|\cdot\|_{H^s(\Omega)}$. If $\mathscr{S}$ is a closed subset of $\mathbb{R}^2$, $C^{0,\delta}(\mathscr{S})$ denotes the space of Hölder continuous functions on $\mathscr{S}$ of order $0 < \delta < 1$.

We define the trace operator γ_0 for $f \in H^s(\Omega)$ as

$$\gamma_0 f(x) = \lim_{r \to 0} \frac{1}{|B(x,r) \cap \Omega|} \int_{B(x,r)\cap\Omega} f(y) \, \mathrm{d}y, \tag{2.11}$$

at every $x \in \overline{\Omega}$ where the limit exists. It is known the the limit (2.11) exists quasi everywhere on $\overline{\Omega}$ with respect to the $(s, 2)$-capacity (see [18]). We point out that $\gamma_0 f \equiv f|_{\partial\Omega}$ for $f \in C(\overline{\Omega})$.

We denote by $C^0(K_n^\xi)$ the space of continuous functions on K_n^ξ, by $C_0(K_n^\xi) := \{\phi \in C^0(K_n^\xi) : \phi(A) = \phi(B) = 0\}$ and by s the one–dimensional measure on K_n^ξ relative to the arc length.

Now we come to the definition of trace spaces on the polygonal curve K_n^ξ. We follow Definition 2.27 in [19] and briefly recall some notations. We define the positive direction on K_n^ξ to be from A to B. Let $V_n^\xi = \{P_1, ..., P_{N+1}\}$ where $P_1 = A$, $P_{N+1} = B$ (A and B are the endpoints of the curve, made of $N+1$ vertices) and $N=4^n$. We denote by l_j, $j=1,...,N$, the sides with endpoints P_j and P_{j+1}, whose length is $L_j=\Pi_{i=1}^n \xi_i^{-1}$. The length of K_n^ξ is $L=\Pi_{i=1}^n 4\xi_i^{-1}$. Since P_1 is the origin, we can associate the arc length $s(P)$ to every point $P\in K_n^\xi$:

$$s(P)=(j-1)\Pi_{i=1}^n \xi_i^{-1}+|P-P_j|, \tag{2.12}$$

if $P\in l_j$ for $j=1,...,N$. Here $|P-P_j|$ is the Euclidean distance between the two points P and P_j. We have a continuous function $\phi_0(s):[0,L]\to\mathbb{R}^2$ that is the parametrization of K_n^ξ by arc length. Moreover, $\phi_0(s)$ is injective and its restriction on each l_j, $j=1,...,N$, is smooth. In addition, we consider the parametrization of the "sub-arc" $\bigcup_{i=j}^N l_i$ by the injective continuous function $\phi_j(s):[0,(N+1-j)L_j]\to\mathbb{R}^2$ such that $\phi_j(0)=P_j$, $j=1,...,N$.

We set $H^s(K_n^\xi)\equiv H^s(\overset{\circ}{K}{}_n^\xi)$ with $\overset{\circ}{K}{}_n^\xi=K_n^\xi\backslash\{A,B\}$, $s\in\mathbb{R}^+$.

Definition 2.2. *For $s>\frac{1}{2}$, the Sobolev spaces $H^s(K_n^\xi)$ and $H_0^1(K_n^\xi)$ are defined by*

$$H^s(K_n^\xi):=\left\{v\in C^0(K_n^\xi):v|_{l_j}\in H^s(\overset{\circ}{l}_j),\quad \overset{\circ}{l}_j=l_j\backslash\{P_j,P_{j+1}\},\quad j=1,...,N\right\},$$

and

$$H_0^1(K_n^\xi):=\left\{v\in C_0(K_n^\xi):v|_{l_j}\in H^1(\overset{\circ}{l}_j),\quad \overset{\circ}{l}_j=l_j\backslash\{P_j,P_{j+1}\},\quad j=1,...,N\right\}.$$

If Ω is a polygon in $\mathbb{R}^2$, then the Sobolev space $H^s(\partial\Omega)$ can be defined in a similar way (see [19]).

We now recall Theorem 2.24 in [19]. For more general details, we refer to [20] and [17].

Proposition 2.1. *Let Ω be a polygon in $\mathbb{R}^2$ with boundary Γ. Let $s>\frac{1}{2}$. Then $H^{s-\frac{1}{2}}(\Gamma)$ is the trace space to Γ of $H^s(\Omega)$ in the following sense:*

(1) γ_0 is a continuous linear operator from $H^s(\Omega)$ to $H^{s-\frac{1}{2}}(\Gamma)$;
(2) there exists a continuous linear operator Ext from $H^{s-\frac{1}{2}}(\Gamma)$ to $H^s(\Omega)$, such that $\gamma_0\circ\mathrm{Ext}$ is the identity operator in $H^{s-\frac{1}{2}}(\Gamma)$.

Finally, we define the weighted Sobolev spaces in a non-convex polygonal domain. Let Q be a non-convex polygonal domain in $\mathbb{R}^2$ with vertices P_j, $j=1,\dots,N$. We denote by θ_j the interior angle of Q at P_j for $j=1,\dots,N$. Let $R=\{1\le j\le N:\theta_j>\pi\}$. Then the set $\{P_j\}_{j\in R}$ is the subset of vertices whose angles θ_j are "reentrant". We choose a suitable constant $\eta>0$. For each $j\in R$, we put $B_\eta(P_j)=\{P\in Q:|P-P_j|<\eta\}$. Let $r:Q\to\mathbb{R}^+$ be a continuous weighting function such that $r(P)=|P-P_j|$ if $P\in B_\eta(P_j)$ for some $j\in R$, and $r(P)=1$ if $P\in Q\backslash\bigcup_{j\in R}B_{2\eta}(P_j)$.

Definition 2.3. *For $\mu \in \mathbb{R}^+$, the weighted Sobolev space $H^{2,\mu}(Q;r)$ is defined by*

$$H^{2,\mu}(Q;r) := \left\{u \in H^1(Q) : r^\mu D^\beta u \in L^2(Q)\ \forall\, |\beta| = 2\right\} \tag{2.13}$$

with the norm

$$\|u\|_{H^{2,\mu}(Q;r)} := \left(\|u\|^2_{H^1(Q)} + \sum_{|\beta|=2} \|r^\mu D^\beta u\|^2_{L^2(Q)} \right)^{\frac{1}{2}}. \tag{2.14}$$

Similarly, for $\mu \in \mathbb{R}^+$, we denote by $\hat{H}^{2,\mu}(Q;\hat{r})$ the weighted Sobolev space where $\hat{r}$ is the distance from the boundary of Q.

3. Existence, uniqueness and regularity results

In this section we introduce the parabolic pre-fractal transmission problem. We refer the reader for details and proofs to [9], see also [21] for the case of an equilateral Koch curve.

Let $\Omega = (0,1) \times (-1,1)$ be the open rectangular domain in $\mathbb{R}^2$. For the sake of clarity, we consider the set $\mathscr{A}$ with only two distinct elements, i.e., $\mathscr{A} = \{\alpha_1, \alpha_2\}$ with $\alpha_1, \alpha_2 \in (2,4)$ and $\alpha_1 < \alpha_2$. Let $n \in \mathbb{N}$ and $\xi \in \mathscr{A}^{\mathbb{N}}$ be fixed. We set $\theta_* = \cos^{-1}\left(\frac{\alpha_1}{2} - 1\right)$ and $\theta^* = \cos^{-1}\left(\frac{\alpha_2}{2} - 1\right)$. Let Ω^1_n and Ω^2_n be the portions of Ω above and below the pre-fractal curve K^ξ_n which from now on will be simply denoted by K_n, whose endpoints are $A = (0,0)$ and $B = (1,0)$. From Figure 3 we can see that there are two reentrant angles for each portion Ω^i_n, which are denoted by θ^i_1 and θ^i_2 for $i = 1,2$. In particular, we have

$$\theta^1_1 = \pi + 2\theta^*, \quad \theta^1_2 = \pi + 2\theta_*, \quad \theta^2_1 = \pi + \theta^*, \quad \theta^2_2 = \pi + \theta_*. \tag{3.1}$$

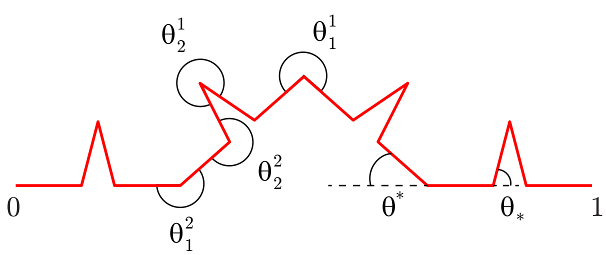

Figure 3: Reentrant angles with $\xi = (3.5, 2.5, \dots)$ and $n = 2$.

In the following we denote by $\theta^1 := \max\{\theta^1_1, \theta^1_2\}$ and by $\theta^2 := \max\{\theta^2_1, \theta^2_2\}$. Let us consider the forms

$$E^{(n)}(u_n, u_n) = \int_\Omega |\nabla u_n|^2 \, \mathrm{d}\mathscr{L}_2 + \int_{K_n} |\nabla_\tau \gamma_0 u_n|^2 \mathrm{d}s, \tag{3.2}$$

defined on the domain

$$V(\Omega, K_n) = \{u_n \in H_0^1(\Omega) : \gamma_0 u_n \in H_0^1(K_n)\} \ . \tag{3.3}$$

In (3.3), $H_0^1(\Omega)$ denotes the usual Sobolev space in Ω and $H_0^1(K_n)$ the trace space. We note that the second integral in the right-hand side of (3.2), the layer energy $E_{K_n}(\cdot,\cdot)$, can be written as the sum of integrals over the segments M of the n-generation:

$$\int_{K_n} |\nabla_\tau \gamma_0 u_n|^2 \, ds = \sum_{M \in F^n} \int_M |\nabla_\tau \gamma_0 u_n|^2 \, ds,$$

where ∇_τ denotes the tangential derivative on M.
The form in (3.2) is not trivial because the domain $V(\Omega, K_n)$ contains the space $H_0^{\frac{3}{2}}(\Omega)$. In fact if $v \in H_0^{\frac{3}{2}}(\Omega)$ then $\gamma_0 v \in H^1(K_n)$. Moreover, both v and $\gamma_0 v$ vanish in A and B; hence $\gamma_0 v \in H_0^1(K_n)$.

Proposition 3.1. *The space $V(\Omega, K_n)$ given by (3.3) is a Hilbert space under the norm*

$$\|u_n\|_{V(\Omega,K_n)} = \left(E^{(n)}(u_n, u_n)\right)^{\frac{1}{2}} . \tag{3.4}$$

Moreover, for each $n \in \mathbb{N}$ $E^{(n)}(\cdot,\cdot)$, with domain $V(\Omega, K_n)$, is a regular, strongly local Dirichlet form in $L^2(\Omega)$.

See [22] and [21] and the references included. We refer to [23] for definitions and main properties of Dirichlet forms.

We now introduce the transmission problem across the pre-fractal layer K_n. In the following, we denote both the functions u_n and their traces $\gamma_0 u_n$ on K_n by the same symbol leaving the interpretation to the context. Let $f(t, P)$ be a given function in $C^{0,\delta}([0, T]; L^2(\Omega))$ with $\delta \in (0, 1)$; we consider the problem $(\overline{P_n})$, formally stated as:

$$(\overline{P_n}) \begin{cases} \frac{\partial u_n(t,P)}{\partial t} - \Delta u_n(t, P) = f(t, P) & \text{in } [0, T] \times \Omega_n^i, \ i = 1, 2, \\ -\Delta_{K_n} u_n(t, P) = \left[\frac{\partial u_n(t,P)}{\partial \nu}\right] & \text{on } [0, T] \times K_n, \\ u_n(t, P) = 0 & \text{on } [0, T] \times \partial\Omega, \\ u_n^1(t, P) = u_n^2(t, P) & \text{on } [0, T] \times \ K_n, \\ u_n(t, P) = 0 & \text{on } [0, T] \times \ \partial K_n, \\ u_n(0, P) = 0 & \text{on } \overline{\Omega}, \end{cases}$$

where u_n^i denotes the restriction of u_n to Ω_n^i, Δ_{K_n} denotes the piecewise tangential Laplacian defined on the layer K_n and $\left[\frac{\partial u_n}{\partial \nu}\right] = \frac{\partial u_n^1}{\partial \nu_1} + \frac{\partial u_n^2}{\partial \nu_2}$ denotes the jump of the normal derivatives across K_n, where ν_i is the inward normal vector to the boundary of Ω_n^i.

In the following, we recall the main results on existence and regularity of the solution to problem $(\overline{P}_n)$. In [21] the existence and uniqueness of the "strict" solution of problem $(\overline{P_n})$ has been proved via a semigroup approach. More precisely, the solvability of the following abstract Cauchy problem, for every fixed $n \in \mathbb{N}$, has been studied:

$$(P_n) \begin{cases} \dfrac{\partial u_n(t)}{\partial t} = A_n\, u_n(t) + f(t), \quad 0 \le t \le T, \\ u_n(0) = 0, \end{cases} \tag{3.5}$$

where $A_n : \mathscr{D}(A_n) \subset L^2(\Omega) \to L^2(\Omega)$ is the generator associated to the energy form $E^{(n)}$,

$$E^{(n)}(u_n, v) = -\int_\Omega A_n u_n v \,\mathrm{d}\mathscr{L}_2, \quad u_n \in \mathscr{D}(A_n), \quad v \in V(\Omega, K_n), \tag{3.6}$$

and T is a fixed positive real number.
A "strict" solution of problem (P_n) is a function

$$u_n \in C^1([0,T];\ L^2(\Omega, m)) \cap\ C([0,T];\ \mathscr{D}(A_n)) \quad \text{s.t.} \tag{3.7}$$
$$\frac{\partial u_n(t)}{\partial t} = A_n u_n(t) + f(t), \quad \text{for every}\ \ t \in [0,T] \quad \text{and}\ \ u_n(0) = 0.$$

Then the following holds.

Theorem 3.1. *Let $0 < \delta < 1,\ f \in C^{0,\delta}([0,T], L^2(\Omega))$, and let*

$$u_n(t) = \int_0^t T_n(t-s)\, f(s)\,\mathrm{d}s \qquad \textit{for every}\ n \in \mathbb{N}, \tag{3.8}$$

where $T_n(t)$ is the analytic semigroup generated by A_n. Then u_n is the unique strict solution of (P_n).
Furthermore there exists $c > 0$, independent from n, such that

$$\|u_n\|_{C^1([0,T],L^2(\Omega))} + \|u_n\|_{C^0([0,T],\mathscr{D}(A_n))} \le c\|f\|_{C^{0,\delta}([0,T],L^2(\Omega))}. \tag{3.9}$$

For the proof, we refer to Theorem 4.3.1 in [24].

Actually, the solution of the abstract Cauchy problem (P_n) is the "strong" solution of problem $(\overline{P_n})$ in the following sense.

Theorem 3.2. *For every given $n \in \mathbb{N}$, let u_n be the solution of problem (P_n). Then we have, for every fixed $t \in [0,T]$,*

$$\begin{cases} \dfrac{\partial u_n(t,P)}{\partial t} - \Delta u_n(t,P) = f(t,P) & \textit{for a.e. } P \in \Omega_n^i,\ i = 1,2, \\ \dfrac{\partial u_n^i}{\partial \nu_i} \in L^2(K_n) & i = 1,2, \\ -\Delta_{K_n} u_n|_{K_n} = \left[\dfrac{\partial u_n}{\partial \nu}\right] & \textit{in } L^2(K_n), \\ u_n(t,P) = 0 & \textit{for } P \in \partial\Omega, \\ u_n(0,P) = 0 & \textit{on}\ \overline{\Omega}, \end{cases} \tag{3.10}$$

where u_n^i is the restriction of u_n to Ω_n^i, $\left[\frac{\partial u_n}{\partial \nu}\right] = \frac{\partial u_n^1}{\partial \nu_1} + \frac{\partial u_n^2}{\partial \nu_2}$ is the jump of the normal derivatives across K_n, ν_i, for $i = 1, 2$, are the inward normal vectors and Δ_{K_n} is the piecewise tangential Laplacian associated to the Dirichlet form E_{K_n}. Moreover $\frac{\partial u_n^i}{\partial \nu_i} \in C([0,T]; L^2(K_n))$, $i = 1, 2$.

For the proof, see Theorems 3.2 and 3.3 in [9].

We recall an important regularity result for the restrictions u_n^i of the solution u_n.

Theorem 3.3. *For every fixed $t \in [0,T]$ $u_n^1 \in \hat{H}^{2,\mu_1}(\Omega_n^1)$, $\mu_1 > \frac{2\theta^1}{\pi+2\theta^1}$, $u_n^2 \in \hat{H}^{2,\mu_2}(\Omega_n^2)$, $\mu_2 > \frac{2\theta^2}{\pi+2\theta^2}$.*

For the proof we refer to Theorem 3.4 in [9].

We remark that from Theorem 3.2 it follows that, for each $t \in [0,T]$, $u_n|_{K_n} \in H^2(K_n)$ and $u_n \in C^0(\overline{\Omega})$ (see Remark 3.1 in [9]). By proceeding as in Theorem 4.2 of [25], with the obvious changes, one can prove that

$$u_n^i \in H^{2,\mu_i}(\Omega_n^i),\ \mu_i > \frac{2\theta^i}{\pi + 2\theta^i},$$

where the weight is the distance from the reentrant vertices (see Definition 2.3).

4. Numerical approximation of problem $(\overline{\mathscr{P}})$

In this section we investigate the main issues concerning the numerical approximation of problem $(\overline{\mathscr{P}})$.

We remark that, since the domains Ω_n^i, $i = 1, 2$ are non-convex polygonal domains, in order to obtain an optimal rate of convergence it will be necessary to generate an appropriate mesh satisfying the conditions of the following Theorem 4.1 (see Appendix Appendix A for details on the mesh algorithm).

Let $\mathscr{D}$ denote the domain Ω_n^i, $i = 1, 2$, and let $\alpha = \alpha_i$, $i = 1, 2$ and $r = r_n^i(x)$ be as in (A.1). Let u_n be the solution of problem (3.10) and u_n^i the restriction of u_n to Ω_n^i. We recall that u_n is in $C^0(\overline{\Omega})$. We denote by $X_h := \{v \in C^0(\mathscr{D}) : v|_S \in \mathbb{P}_1, \forall\ S \in \mathscr{T}_{n,h}^{\xi}\}$, where $\mathbb{P}_1$ denotes the set of polynomial functions of degree one. Let $I_h : H^{2,\alpha}(\mathscr{D}) \to X_h$ be the X_h-interpolating operator, defined as follows : $I_h(u_n)|_S \in \mathbb{P}_1$ for every $S \in \mathscr{T}_{n,h}^{\xi}$ and $I_h(u_n) = u_n$ at any vertex of any $S \in \mathscr{T}_{n,h}^{\xi}$. We note that the interpolation operator is well defined since $u_n \in C^0(\overline{\Omega})$. In the above notations and assumptions we have for each $t \in [0,T]$:

Theorem 4.1. *Let $\{\mathscr{T}_{n,h}^{\xi}\}$ be a family of meshes over $\mathscr{D}$ satisfying conditions from (a) to (f) in Appendix Appendix A. Then there exists a constant $C > 0$, independent from h, such that*

$$|u_n^i - I_h(u_n^i)|_{H^1(\Omega_n^i)} \leq C\, h \left\{ \sum_{|\beta|=2} \| r^{\alpha_i} \cdot D^{\beta} u_n^i \|^2_{L^2(\Omega_n^i)} \right\}^{1/2}. \tag{4.1}$$

In the following for simplicity we will drop the superscript ξ. With the symbol $\mathscr{T}^i_{n,h_i}$ we will denote the triangulation over the subdomain Ω^i_n. Since Ω is divided by K_n into two subdomains Ω^1_n and Ω^2_n, which are non-convex polygonal domains having K_n as a portion of the boundary, we generate an appropriate mesh $\mathscr{T}^i_{n,h_i}$, $i = 1, 2$, satisfying the requirements to apply the mesh algorithm (see Appendix Appendix A) and the natural triangulation over $\overline{\Omega}$ is

$$\mathscr{T}_{n,h} = \mathscr{T}^1_{n,h_1} \bigcup \mathscr{T}^2_{n,h_2}, \tag{4.2}$$

where $h = \max\{h_1, h_2\}$ and $\sigma = \max\{\sigma_1, \sigma_2\}$.

Under these conditions, the size of the elements is consistent with the assumptions of Theorem 4.1, thus, by proceeding as in Proposition 4 and Theorem 5.1 in [8], one can deduce a $V(\Omega, K_n)$-estimate and a $L^2(\Omega^i_n)$-estimate of the linear interpolation error for any function which has $H^{2,\mu}$-regularity, $\mu \in (0, 1)$.

With these two properties at hand, the numerical approximation of the problem $(\overline{P_n})$ is carried out in two steps.

In the first step the semi-discrete problem is obtained by discretizing with a Galerkin method the space variable only and the following a priori error estimate of the order of convergence holds.

Theorem 4.2. *Let $u_n(t)$ be the solution of $(\overline{P_n})$, $u^i_n(t)$ be the restriction to Ω^i_n of $u_n(t)$, for $i = 1, 2$, and $u_{n,h}(t)$ be the semi-discrete solution. For each $t \in [0, T]$, it holds*

$$\|u_n(t) - u_{n,h}(t)\|_2^2 + \int_0^t \|u_n(\tau) - u_{n,h}(\tau)\|^2_{V(\Omega,K_n)} \,\mathrm{d}\tau \leq ch^2 \left(\int_0^t \|f(\tau)\|_2^2 \,\mathrm{d}\tau \right) \tag{4.3}$$

where c is a suitable constant independent of h.

For the proof one can proceed as in Theorem 5.2 of in [8] with the obvious changes.

In the second step, the fully discretized problem is obtained by applying a finite difference scheme, the so-called θ-method, on the time variable. As it is well-known, the θ-scheme is unconditionally stable with respect to the $L^2(\Omega)$-norm provided that $\frac{1}{2} \leq \theta \leq 1$. On the contrary, in the case of $0 \leq \theta < \frac{1}{2}$, one has to assume that $\{\mathscr{T}_{n,h}\}$ is a quasi-uniform family of triangulations and that a restriction on the time step holds. Since the peculiarity of our mesh $\{\mathscr{T}_{n,h}\}$ is not to be quasi-uniform, from now on we assume $\frac{1}{2} \leq \theta \leq 1$. An error estimate between the semi-discrete solution $u_{n,h}(t_l)$ and the fully discrete one $u^l_{n,h}$ can be obtained as in Theorem 6.1 in [8]. From this estimate and Theorem 4.2 we deduce the following convergence result.

Theorem 4.3. *Let $t_l = l\Delta t$ for $l = 0, 1, \ldots, \mathscr{M}$, $\Delta t > 0$ being the time step and $\mathscr{M}$ being the integer part of $T/\Delta t$. Let $f \in C^{0,\delta}([0, T]; L^2(\Omega))$ and $\frac{\partial f}{\partial t} \in L^2([0, T] \times \Omega, \mathrm{d}t \times \mathrm{d}\mathscr{L}_2)$. Let n be fixed and let $u_n(t)$ be the solution of problem $(\overline{P_n})$, $u^l_{n,h}$ be the fully discretized solution as given by the θ-method with $\frac{1}{2} \leq \theta \leq 1$. Then*

$$\|u_n(t_l) - u^l_{n,h}\|_2^2 \leq ch^2 \left(\int_0^T \|f(\tau)\|_2^2 \,\mathrm{d}\tau \right) + C_\theta \triangle t^2 \left(\|f(0)\|_2^2 + \int_0^T \left\| \frac{\partial f}{\partial \tau}(\tau) \right\|_2^2 \mathrm{d}\tau \right),$$

where c is the constant given by Theorem 4.2 and C_θ is a constant independent from $\mathscr{M}$, Δt and h.

5. The layer optimization problem ($\mathscr{P}$)

In this section we describe how to approximate numerically problem ($\mathscr{P}$). Since it is too complex to be solved directly, we approach the solution to problem ($\mathscr{P}$) by iteratively solving a sequence of simpler optimization problems $\{(\mathscr{P}_n)\}$ driven by a heuristic method.

First, we assume that the optimal solution K^* exists. Therefore, the solution to problem ($\mathscr{P}$) is an element of $\mathscr{K}$. Since every element of $\mathscr{K}$ can be obtained through an iterative growth process starting from a flat segment K_0 (as shown in Section 2.1), we can state that there exists an iterative growth "dynamics" that links K_0 with K^*.

With this aim, we define a mapping denoted by $\Phi^{i,\alpha}$ that represents a growth dynamics for the evolution of one particular segment of the layer, indexed by i, by applying a contraction factor α^{-1}. In particular, given a layer K_n formed by a union of S_n segments, i.e. $K_n = \cup_{i=1}^{S_n} M_i$, the mapping $\Phi^{i,\alpha}$ is defined as:

$$\Phi^{i,\alpha}(K_n) = M_1^n \cup \cdots \cup \varphi^\alpha(M_i^n) \cup \cdots \cup M_{S_n}^n, \quad i = 1, \ldots, S_n,\ \alpha \in [2+\epsilon, 4].$$

For every given iteration n, it is necessary to select which segment grows. This selection comes from an heuristic method. In particular, we choose the segment of the layer which has the maximum heat flux, defined as:

$$\phi(M_i) = \int_{M_i} -\lambda \left[\frac{\partial u_n}{\partial \nu}\right] \mathrm{d}s.$$

The idea behind this heuristic is the following: as the goal is to minimize the maximum temperature in the domain, we look for the most uniform temperature distribution. Therefore, we apply a change to the segment which has the maximum heat flux. We denote by i_n^* the index of such segment and we define it by

$$i_n^* = \arg\max_{i \in \mathscr{B}_n} \phi(M_i),$$

where $\mathscr{B}_n$ is the set of indices of segments that can grow, which is defined by:

$$\mathscr{B}_n = \left\{ j_n \in \mathbb{N} : \left\{ \begin{array}{ll} j_n \in \mathscr{B}_{n-1} \setminus \{i_{n-1}^*\} & \text{if} \quad K_n = K_{n-1} \\ j_n \in \{1, \ldots, S_n\} & \text{otherwise} \end{array} \right. \right\}$$

This set is formed by all indices from 1 to S_n except the case when the layer has not grown in the previous iteration. This happens when the optimal contraction factor for the segment $M_{i_{n-1}^*}$ with maximum flux in the previous iteration is 4. This means that this segment does not grow, the layer remains the same ($K_n = K_{n-1}$) and therefore the segment has to be removed for growing purposes in the current iteration n. In particular, the optimal contraction factor for segment i_n^* is denoted by α^* and it is the solution of the following optimization problem $(\mathscr{P}_n)$:

$$(\mathscr{P}_n) \qquad \alpha^* = \inf_{\alpha\in[2+\epsilon,4]} \left(\max_{P\in\Omega} u\left(T, P, \Phi^{i_n^*,\alpha}(K_n)\right) \right)$$

where $u\left(T, P, \Phi^{i_n^*,\alpha}(K_n)\right)$ is the solution of the problem $\overline{\mathscr{P}_n}$ with interface $\Phi^{i_n^*,\alpha}(K_n)$. Since the steady state is only reached when $t \to +\infty$, for application purposes we define T as the finite time in which all variables of the process do not vary anymore in significant way (for instance the 99% of their final value, which is theoretically computable).

Therefore, as long as $\mathscr{B}_n \neq \emptyset$, the growth dynamics is given by:

$$\begin{cases} \mathscr{B}_0 = \{1\},\ i_0^* = 1,\ K_0 = [0,1], \\ K_{n+1} = \Phi^{i_n^*,\alpha^*}(K_n),\ i_n = 1, 2, \dots \end{cases}$$

The dynamics stops when $\mathscr{B}_n = \emptyset$, i.e. no segment grows.

The approach described above can be resumed in Algorithm 1 below. This algorithm includes some variations, which have been added for computational and application purposes. First, given an iteration n, the optimal contraction factor α^* for the segment $M_{i_{n-1}^*}$ with highest flux is selected from a discrete set of z different factors $\{\alpha_1, \alpha_2, \dots, \alpha_z\}$. This procedure does not guarantee that the factor α obtained is the optimal, but it is necessary to computationally approach the problem given its complexity. Furthermore, $\alpha_j < 4, j = 1, 2, \dots, z$, because applying a contraction factor of 4 does not produce any change in the layer from a computational point of view.

Finally, the layer evolves if the relative difference of temperature between the maximum temperature u_{max} with the current layer K_n and the maximum temperature u_{max}^{prov} with the provisional layer $K_{j^*}^{prov}$ evaluated is greater than a threshold $\delta > 0$. This threshold ensures that the layer evolves only if the reduction of maximum temperature is enough to justify the increase of length of the layer.

6. Numerical results

In this section we study the growth of the pre-fractal layer and its final configuration depending on the heat source position and the layer conductivity. The dimensional equations of the problem are, for every $t \in [0, T]$,

$$\begin{cases} \rho\ C_p\ \dfrac{\partial u}{\partial t} = \lambda_b\ \Delta u + f & \text{in } L^2(\Omega), \\ -\lambda_s \Delta_{K_n} u = \lambda_b \left[\dfrac{\partial u}{\partial \nu}\right] & \text{in } L^2(K_n), \\ u(0, x) = 0 & \forall\, x \in \overline{\Omega}, \\ u(t, x) = 0 & \forall\, x \in \partial\Omega, \end{cases}$$

where

Data: $\{\alpha_1, \alpha_2, \ldots, \alpha_z\} \in [2+\epsilon_1, 4-\epsilon_2], \delta, \Omega = (1,0)\times(-1,1), \lambda, f, K_0 = \{(0,0),(1,0)\}, \mathscr{B}_0 = \{1\}, i_0^* = 1, n = 0$
Result: K
Obtain $u_{K_0}(T,P), \forall P \in \Omega$;
$u_{max} \leftarrow \max_{P\in\Omega} u_{K_0}(T,P)$;
while $\mathbf{card}(\mathscr{B}_n) \neq 0$ **do**
  if $n > 0$ **then**
    for $i \in \mathscr{B}_n$ **do**
      Obtain $\phi(M_i)$;
    end
    $i_n^* \leftarrow \arg\min_{i\in\mathscr{B}_n} \phi(M_i)$;
  end
  for $j \in \{1,2,\ldots,z\}$ **do**
    $K_j^{prov} = \Phi^{i_n^*,\alpha_j}(K_n)$;
    Obtain $u_{K_j^{prov}}(T,P), \forall\, P \in \Omega$;
  end
  $j^* \leftarrow \arg\min_{j=1,2,\ldots,z}\Big(\max_{P\in\Omega} u_{K_j^{prov}}(T,P)\Big)$;
  $u_{max}^{prov} \leftarrow \max_{P\in\Omega} u_{K_{j^*}^{prov}}(T,P)$
  if $\frac{u_{max}-u_{max}^{prov}}{u_{max}} > \delta$ **then**
    $K_{n+1} \leftarrow K_{j^*}^{prov}$;
    $\mathscr{B}_{n+1} \leftarrow \{1,2,\ldots,\mathbf{card}(\mathscr{B}_n)+3\}$;
    $u_{max} \leftarrow u_{max}^{prov}$;
  else
    $K_{n+1} \leftarrow K_n$;
    $\mathscr{B}_{n+1} \leftarrow \mathscr{B}_n \setminus \{i_n^*\}$
  end
  $n \leftarrow n+1$;
end
$K \leftarrow K_n$

Algorithm 1: Algorithm to approach solution K^* for problem $(\mathscr{P})$

- ρ is the material density in the bulk Ω (in Kg/m^3);
- C_p is the heat capacity at constant pressure (in J/(Kg $\cdot$ °C));
- λ_b is the thermal conductivity in the bulk domain Ω (in W/(m $\cdot$ °C));
- λ_s is the thermal conductivity in the pre-fractal layer K_n (in W/°C));
- the term f represents a thermal source (in W/m^3);
- u is the unknown variable: the temperature in Celsius degrees.

In order to preserve dimensional coherence, we assume that Ω is a planar section of a three-dimensional domain of infinite depth. Moreover, we consider that the layer K_n has an infinitesimal thickness on the planar section.

From this point on, the values of the parameters and variables defined above are referred to their mentioned units. Table 1 shows the values consistently used for ρ, C_p and λ_b in all subsections. On the other hand, in Algorithm 1, the contraction factors are set to $\alpha_i = 0.19(i-1) + 2.1, i = 1, \ldots, 11$, and the treshold is set to $\delta = 0.01$.

ρ	C_p	λ_b
8000	450	1

Table 1: Numerical values used in the simulations for the physical coefficients

6.1. Iterative growth of the pre-fractal layer

In this subsection we examine how the layer grows to maximize the heat draining. In particular, the evolution of the layer according to the iterative growth dynamics represented by $\Phi^{i,\alpha}$ and obtained through Algorithm 1 is shown in Figure 4. In this figure, we observe how the layer is iteratively approaching the center of the heat source. This is due firstly to the fact that the segments with the maximum flux, and therefore the segments that grow first, are the ones closer to the heat source, and secondly to the fact that the optimal contraction factors for these segments are the ones that approach the layer to the heat source.

These results are sensible from a physical point of view. The layer is more conductive than the bulk and is connected in its extremes to the walls which are at a constant temperature of 0 °C. This implies that the layer constitutes a more efficient path for heat draining than the bulk. In addition, the greater the temperature gradient between the bulk and the layer, the greater the heat flux along the layer. Therefore, the closer the layer is to the points of maximum temperature in the bulk, the more efficiently the heat is drained.

Nevertheless, the growth towards the heat source must be balanced with the increase of length of the layer. When the layer grows, so does the distance between some points of the layer and the extremes connected to the walls. Therefore, the resistance to heat flow along the layer increases. This implies that it is not effective to grow the layer everywhere; it is physically more convenient to grow only the parts close enough to the heat source (and therefore to the areas of high temperature in the bulk), in order to outweigh the effect of increasing its length. This phenomenon can be observed in Figure 4, where the layer does not grow in the parts that are farther from the heat source.

The numerical results shown in Figure 4 were obtained using $f(x, y) = 3000 \exp(-5(x - 0.3)^2 - 5(y - 0.4)^2)$ and $\lambda_s = 1000$.

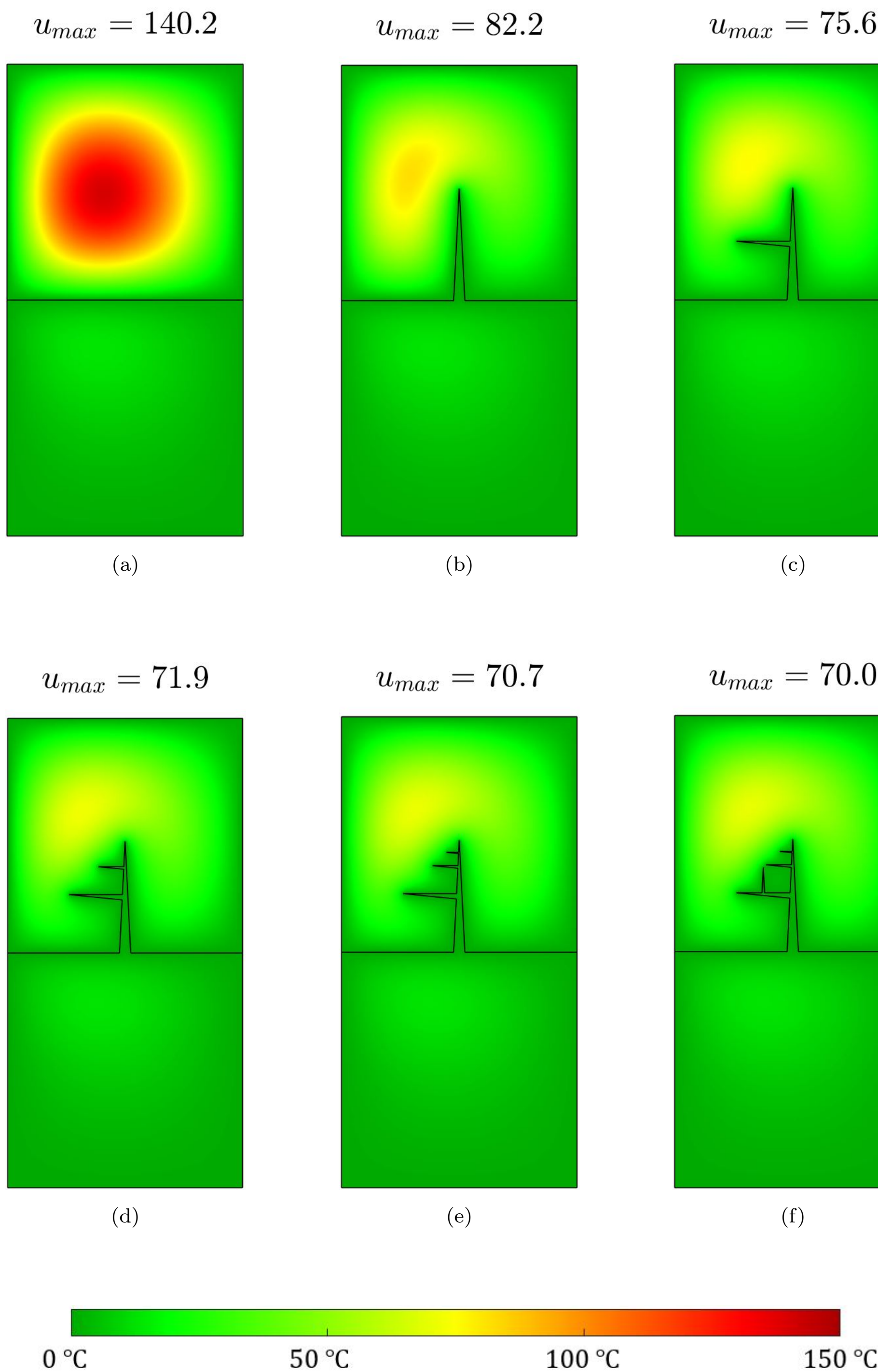

Figure 4: Iterative growth of the pre-fractal Koch mixture layer to produce the maximum reduction of temperature (4a - 4f), maximum temperature u_{max} in each bulk and temperature colormap.

6.2. Dependence on the heat source position

In this subsection we analyze how the position of the heat source affects the shape of the pre-fractal layer according to Algorithm 1 (see Figure 5). When the heat source is centered, the layer grows a spike in the center of the layer and then stops growing (see Figure 5a). This is because further growing does not benefit heat draining, as the increase of length does not translate into an approach to the heat source. On the other hand, when the heat source is displaced from the center, the layer begins to grow further to approach the heat source (see Figures 5b - 5g). In fact, when the heat source center is located near to the walls, the layer grows a second spike (see Figures 5h - 5j) and the central spike even flattens (see Figure 5j). These results are sensible from a physical point of view as in Subsection 6.1.

The numerical results shown in Figure 5 were obtained using $f(x,y) = 3000\exp(-5(x-x_0)^2 - 5(y-y_0)^2)$, where x_0 and y_0 vary from Figure 5a to 5j, and $\lambda_s = 1000$.

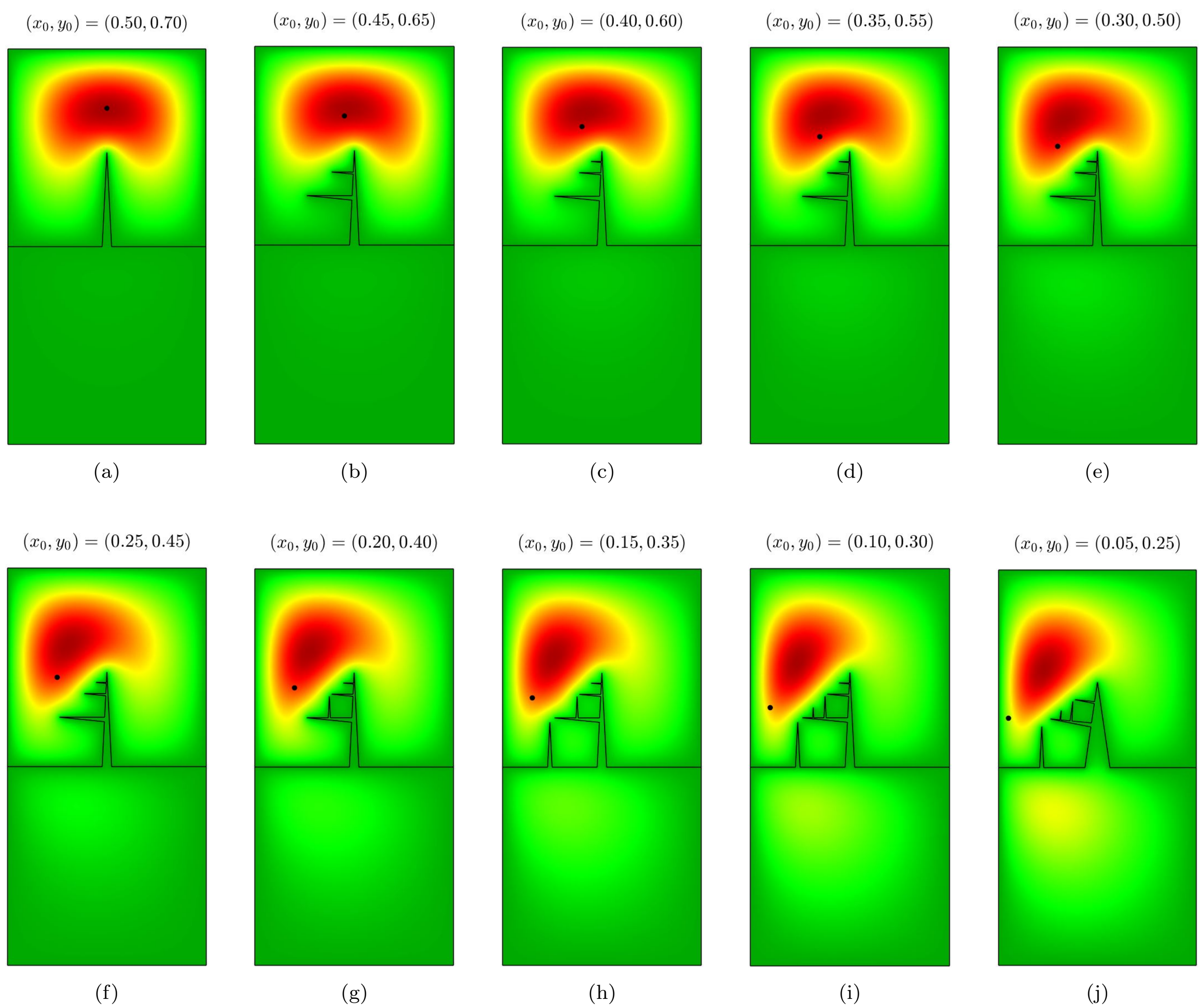

Figure 5: Dependence of the pre-fractal Koch mixture layer on the heat source position center (x_0, y_0) to produce the maximum reduction of temperature.

6.3. *Dependence on the conductivity λ_s*

In this subsection we study the influence of the the layer conductivity λ_s on the shape of the pre-fractal obtained through Algorithm 1 (see Figure 6). In this figure we observe that, the higher the conductivity, the greater the growth of the pre-fractal and the closer it is to the heat source (see Figures 6a - 6d).

This result is sensible from a physical point of view. The heat flux along the layer is directly proportional to the conductivity of the layer and the bulk-layer temperature gradient. This means that, given two layers 1 and 2 with conductivity values λ_1 and λ_2 respectively, $\lambda_1 < \lambda_2$, the bulk-layer temperature gradient for layer 1 must be larger than for layer 2 to obtain the same heat flux value. This implies that layer 1 must reach areas of higher bulk temperature than layer 2, i.e., layer 1 must grow more than layer 2. However, this means that the resistance of layer 1 is higher than that of layer 2. Therefore, the growth of layer 1 is more penalized than that of layer 2 to obtain the same heat flux and hence, the lower the conductivity, the lower the growth of the layer.

The numerical results shown in Figure 6 were obtained using $f(x, y) = 3000 \exp(-5(x - 0.65)^2 - 5(y - 0.35)^2)$.

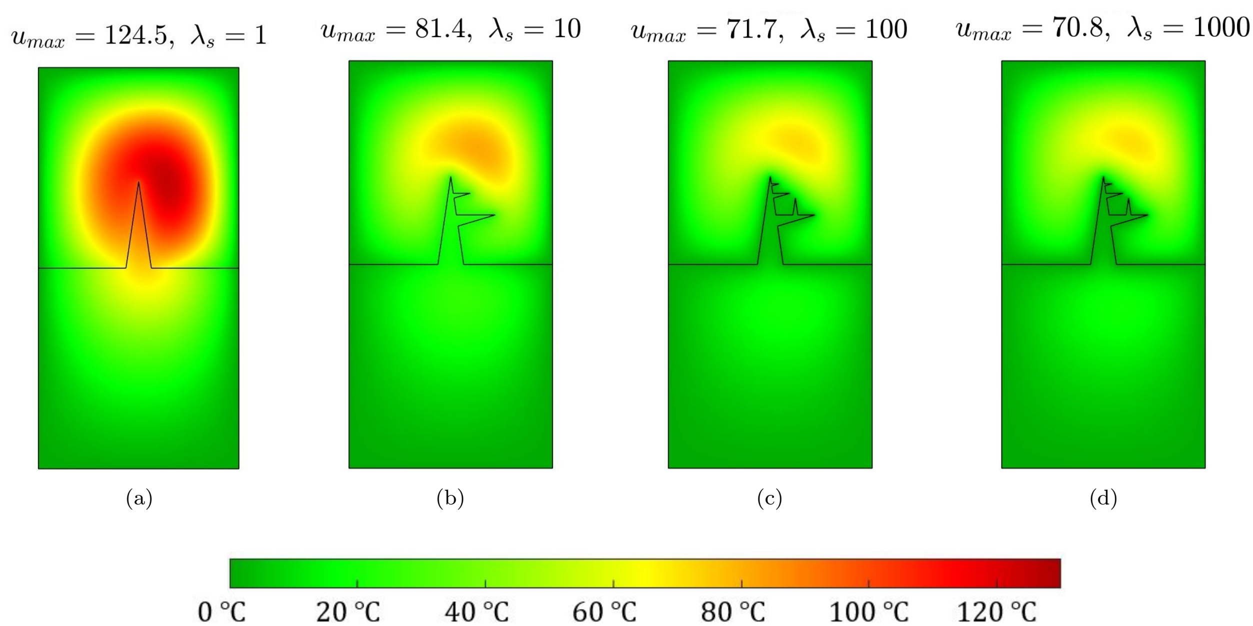

Figure 6: Pre-fractal Koch mixture that produces the maximum reduction of temperature with conductivity $\lambda_s = 1$ (6a), $\lambda_s = 10$ (6b), $\lambda_s = 100$ (6c) and $\lambda_s = 1000$ (6d), maximum temperature u_{max} in each bulk and temperature colormap.

7. Conclusions and open problems

Not all pre-fractal layers are suitable for draining heat purposes. As we show in Section 6, the optimal growth dynamics of a pre-fractal Koch-mixture generates pre-fractals which have grown only in those areas closest to the heat source. This is the balance between two opposite effects produced when a highly conductive thin layer grows: i) the layer moves closer to the heat source and is located in higher temperature areas of the bulk to increase the bulk-layer temperature gradient; ii) the layer increases its length and thus its resistance to heat transfer. For this reason, pre-fractal growth is only desirable in areas of the bulk whose temperature implies a gradient that outweighs the increase in resistance (see Figures 4 and 5). The extent of these areas depends on the conductivity of the layer itself: the lower the conductivity, the higher the temperature and subsequent gradient required to produce the same heat flux and thus the lower the extent of these areas and the growth of the pre-fractal (see Figure 6).

The conclusions obtained lead to the question of what type of layer, fractal or not, improves the performance of Koch-mixture fractals. The geometry of these mixtures implies that their maximum is in the center, which makes them inefficient in problems where the heat source is not centered, being preferable a layer whose geometry depends on the position of the heat source to approach it as close as possible. In addition, the infinite-length property of fractals is counterproductive in those parts far from the highest temperature areas. For this reason, in future works we will study the heat-draining capability of layers whose geometry is oriented towards the heat source and which also only develop fractal structure in their surroundings. Moreover, the results of this paper can be extrapolated to a more realistic 3D problem. In some cases, a 3D fractal surface obtained from an extruded 2D fractal has been shown by simulations to behave similarly to the two-dimensional case. Nevertheless, the general 3D case presents additional challenges that probably require appropriate algorithms and theoretical analysis. The study of the general 3D problem is the object of our current research activity.

The results of this work also lead us to study a problem which may be considered as an evolution of the present one: an automatic control system in which the growth dynamics of a pre-fractal barrier evolves automatically to drain heat from sources in an optimal way. This growth dynamics would be guided by the feedback of thermal flows, according to more or less flexible rules of an asymmetric mixture to adapt to the extemporaneous conditions of any thermal sources located in the bulk. This scenario incredibly lends itself to many applications of practical interest. For example, a highly conductive layer could be made with deformable material and installed on electronic boards in which it is of particular interest to drain heat optimally from variable thermal sources (for instance, microchips or other electronic components which are activated and heat up with their usage). In particular, the electronic devices (micro actuators) would guide the fractal dynamics of the barrier on the basis of the measurement of the thermal field on the electronic board and/or of thermal fluxes. We remark that in the formulation of the problem some functional constraints could be introduced, such as constraints on the maximum length of the pre-fractal or temperature constraints on some points of the barrier. The inclusion of constraints in the optimization problem makes the logic of the optimization algorithm more complex and is one of the objects of forthcoming papers.

Appendix A. Appendix: The mesh algorithm

In this section we recall the mesh algorithm developed in [10], which is crucial in order to obtain an optimal rate of convergence of the numerical solution. Here, $n \in \mathbb{N}$ and $\xi \in \mathscr{A}^{\mathbb{N}}$ are fixed.

We denote by $\mathscr{Q}$ the set of all reentrant corners. From Theorem 3.3, we have that the solution is singular at these reentrant corners, indeed it is not in $H^2(\Omega_n^i)$ as in the case of smooth boundaries, and, as it is well known, this lack of regularity deteriorates the rate of convergence in the numerical approximation.

In view of these singularities, in order to get an optimal rate of convergence for the finite element approximations, the triangulation of the domains Ω_n^i must be suitably refined according to the conditions introduced by Grisvard in [20] (see conditions (c) and (d) below). To this aim, a first crucial requirement is to ask that all the vertices of V_n^ξ are nodes of the family of triangulations $\{\mathscr{T}_{n,h}^\xi\}$.

We ask that the mesh refinement process generates a family of triangulations $\{\mathscr{T}_{n,h}^\xi\}$ with the following properties:

(a) any $\mathscr{T}_{n,h}^\xi$ is *conformal*;

(b) the family of triangulations $\{\mathscr{T}_{n,h}^\xi\}$ is *regular*;

(c) $h_S \leq \sigma h^{\frac{1}{1-\mu_i}}$ for every triangle $S \in \mathscr{T}_{n,h}^\xi$ having at least one reentrant vertex in $\mathscr{Q}$, where:
  - -) h is the mesh size, i.e., $h = \max_{S\in\mathscr{T}_{n,h}^\xi} h_S$;
  - -) h_S is the diameter of the triangle $S \in \mathscr{T}_{n,h}^\xi$, defined as the length of its longest edge;
  - -) σ is the regularity constant of the mesh, defined as $h_S/\rho_S \leq \sigma$, $\forall S \in \{\mathscr{T}_{n,h}^\xi\}$, where ρ_S is the radius of the biggest circle inscribed in S;
  - -) μ_i is given in Theorem 3.3;

(d) $h_S \leq C\sigma h \inf_{x\in S}[r_n^i(x)]^{\mu_i}$ for any other triangle $S \in \mathscr{T}_{n,h}^\xi$, where:
  - -) C is a constant greater than 1;
  - -) $r_n^i(x)$ is the so-called weighting distance, defined as

$$r_n^i(x) = \begin{cases} |x-P| & \text{if } x \in B_{\eta_n}(P) \text{ for some } P \in \mathscr{Q} \\ 1 & \text{if } x \notin \bigcup_{P\in\mathscr{Q}} B_{2\eta_n}(P) \\ \frac{1-\eta_n}{\eta_n}(|x-P|-\eta_n)+\eta_n & \text{otherwise ;} \end{cases} \tag{A.1}$$

  - -) η_n is equal to a quarter of the shortest distance between any pair of points in $\mathscr{Q}$;

(e) the mesh size $h \to 0$ when the iteration number of the mesh algorithm goes to infinity;

(f) the mesh algorithm produces a sequence of nested refinements, i.e. all the nodes in the current triangulation are also nodes of the one obtained after the refinement.

The first assumption guarantees that the mesh covers exactly the domain Ω and that the set of nodes of each triangulation corresponds to the set of vertices of the triangles. The

second assumption requires that the shape of any triangle is not altered in an unlimited way by the refinement process. This requirement acts as a lower bound of the mesh quality. For the definitions of conformal and regular mesh, we refer e.g. to [26]. Hypotheses (c) and (d) are required to generate a proper decomposition of the domain around the reentrant vertices in order to guarantee an optimal rate of convergence of the numerical solution, and they require that the closest triangles to any reentrant vertex are more refined than those triangles that are far away.
The hypothesis (e) is required to guarantee the convergence of the finite element method. In the end, the hypothesis (f) is a special case of the so-called *h-refinement*, which leads to a more accurate computation of the numerical solution. In particular, it bounds the growth of the complexity of the numerical problems associated to the subsequent refinements.

The algorithm that we use is a mesh refinement algorithm for fractal mixture interfaces and it is an extension of the one in [27]. We remark that the algorithm in [27] produces meshes that do not satisfy the requirements (e) and (f); moreover, the present algorithm allows to tackle transmission problems taking place across more complex interfaces and allows to generate nested refinements.

We now recall the mesh algorithm $\mathscr{I}$ which was introduced in [9]. We summarize the properties of the mesh produced by the algorithm $\mathscr{I}$ in the following theorem.

Theorem Appendix A.1. *Let $n \in \mathbb{N}$ and $\xi \in \mathscr{A}^{\mathbb{N}}$ be given. If $\mathscr{T}^{\xi}_{n,h_0}$ is a coarse mesh of Ω with the following properties:*

- *(i)* $\mathscr{T}^{\xi}_{n,h_0} \cap \Omega^i_{\xi,n}$ *is a triangulation of* $\Omega^i_{\xi,n}$ *for* $i = 1, 2$*;*
- *(ii)* $\mathscr{T}^{\xi}_{n,h_0}$ *is shape regular with aspect ratio* σ*;*
- *(iii)* $h_0 < \frac{1}{2} - \eta_1$*,*

then we can apply the algorithm $\mathscr{I}$ on $\mathscr{T}^{\xi}_{n,h_0}$ and generate a family of triangulations $\{\mathscr{T}^{\xi}_{n,h}\}$ of Ω which satisfies the properties from (a) to (f) introduced at the beginning of this Appendix.

Acknowledgments

S. C. and M. R. L. have been supported by the Gruppo Nazionale per l'Analisi Matematica, la Probabilità e le loro Applicazioni (GNAMPA) of the Istituto Nazionale di Alta Matematica (INdAM). J. R. was supported by Universidad Politécnica de Madrid as part of the UPM-Funded Research, Development and Innovation Programme.
This work was undertaken while J. R. was visiting the Department of Basic and Applied Sciences for Engineering of Sapienza Università di Roma.

References

[1] M. Filoche, B. Sapoval, Transfer across random versus deterministic fractal interfaces, Phys. Rev. Lett. 84 (2000) 5776–5779.

[2] B. Sapoval, General formulation of laplacian transfer across irregular surfaces, Phys. Rev. Lett. 73 (1994) 3314–3316. doi:10.1103/PhysRevLett.73.3314.
URL http://link.aps.org/doi/10.1103/PhysRevLett.73.3314

[3] D. B. Tuckerman, R. F. W. Pease, High-performance heat sinking for vlsi, Electron Device Letters, IEEE 2 (5) (1981) 126 –129. doi:10.1109/EDL.1981.25367.

[4] Y. Chen, P. Cheng, Heat transfer and pressure drop in fractal tree-like microchannel nets, International Journal of Heat and Mass Transfer 45 (13) (2002) 2643 – 2648. doi:10.1016/S0017-9310(02)00013-3.
URL http://www.sciencedirect.com/science/article/pii/S0017931002000133

[5] D. V. Pence, Reduced pumping power and wall temperature in microchannel heat sinks with fractal-like branching channel networks, Microscale Thermophysical Engineering 6 (4) (2003) 319–330.

[6] H. Wang, X. Chen, Performance improvements of microchannel heat sink using koch fractal structure and nanofluids, in: Structures, Vol. 50, Elsevier, 2023, pp. 1222–1231.

[7] W. Chen, Z. Men, S. Liu, Fast parameterized fractal modeling of active heat transfer channel, Applied Thermal Engineering 209 (2022) 118297.

[8] M. Cefalo, G. Dell'Acqua, M. R. Lancia, Numerical approximation of transmission problems across koch-type highly conductive layers, Applied Mathematics and Computation 218 (9) (2012) 5453 – 5473. doi:10.1016/j.amc.2011.11.033.
URL http://www.sciencedirect.com/science/article/pii/S0096300311013634

[9] M. Cefalo, M. R. Lancia, H. Liang, Heat-flow problems across fractals mixtures: regularity results of the solutions and numerical approximation, Differential Integral Equations 26 (9–10) (2013) 1027–1054.

[10] M. Cefalo, M. R. Lancia, An optimal mesh generation for domains with koch-type boundaries, Math. Comput. Simulation 106 (2014) 133–162.

[11] M. Cefalo, S. Creo, M. R. Lancia, P. Vernole, Nonlocal venttsel' diffusion in fractal-type domains: regularity results and numerical approximation, Math. Methods Appl. Sci. 42 (14) (2019) 4712–4733.

[12] M. Cefalo, S. Creo, M. Gallo, M. R. Lancia, P. Vernole, Approximation of 3D Stokes flows in fractal domains, in: Fractals in Engineering: Theoretical Aspects and Numerical Approximations, ICIAM 2019 SEMA SIMAI Springer Ser., 8, Springer-Cham, 2021.

[13] S. Creo, M. Hinz, M. R. Lancia, A. Teplyaev, P. Vernole, Magnetostatic problems in fractal domains, in: Fractals and Dynamics in Mathematics, Sciences and the Arts Volume 5, Analysis, Probability and Mathematical Physics on Fractals, World Scientific, 2020.

[14] U. Mosco, Harnack inequalities on scale irregular Sierpinski gaskets, in: Nonlinear problems in mathematical physics and related topics, II, Vol. 2 of Int. Math. Ser. (N. Y.), Kluwer/Plenum, New York, 2002, pp. 305–328. doi:10.1007/978-1-4615-0701-7_17.
URL http://dx.doi.org/10.1007/978-1-4615-0701-7_17

[15] U. Mosco, An elementary introduction to fractal analysis, in: Nonlinear analysis and applications to physical sciences, Springer Italia, Milan, 2004, pp. 51–90.

[16] M. T. Barlow, B. M. Hambly, Transition density estimates for Brownian motion on scale irregular Sierpinski gaskets, Ann. Inst. H. Poincaré Probab. Statist. 33 (5) (1997) 531–557. doi:10.1016/S0246-0203(97)80104-5.
URL http://dx.doi.org/10.1016/S0246-0203(97)80104-5

[17] J. Nečas, Les méthodes directes en théorie des équations elliptiques, Masson et Cie, Éditeurs, Paris, 1967.

[18] D. R. Adams, L. I. Hedberg, Function spaces and potential theory, Vol. 314 of Grundlehren der Mathematischen Wissenschaften [Fundamental Principles of Mathematical Sciences], Springer-Verlag, Berlin, 1996.

[19] F. Brezzi, G. Gilardi, Finite elements mathematics, in: H. Kardestuncer, D. H. Norrie: Finite Element Handbook, McGraw-Hill Book Co., New York, 1987.

[20] P. Grisvard, Elliptic problems in nonsmooth domains, Vol. 24 of Monographs and Studies in Mathematics, Pitman (Advanced Publishing Program), Boston, MA, 1985.

[21] M. R. Lancia, P. Vernole, Irregular heat flow problems, SIAM J. Math. Anal. 42 (4) (2010) 1539–1567. doi:10.1137/090761173.
URL http://dx.doi.org/10.1137/090761173

[22] M. R. Lancia, P. Vernole, Convergence results for parabolic transmission problems across highly conductive layers with small capacity, Adv. Math. Sci. Appl. 16 (2) (2006) 411–445.

[23] M. Fukushima, Y. Oshima, M. Takeda, Dirichlet forms and symmetric Markov processes, Vol. 19 of de Gruyter Studies in Mathematics, Walter de Gruyter & Co., Berlin, 1994.

[24] A. Lunardi, Analytic semigroups and optimal regularity in parabolic problems, Progress in Nonlinear Differential Equations and their Applications, 16, Birkhäuser Verlag, Basel, 1995.

[25] M. R. Lancia, U. Mosco, M. A. Vivaldi, Homogenization for conductive thin layers of pre-fractal type, J. Math. Anal. Appl. 347 (1) (2008) 354–369. doi:10.1016/j.jmaa.2008.06.011.
URL http://dx.doi.org/10.1016/j.jmaa.2008.06.011

[26] A. Quarteroni, A. Valli, Numerical approximation of partial differential equations, Vol. 23 of Springer Series in Computational Mathematics, Springer-Verlag, Berlin, 1994.

[27] R. D. Wasyk, Numerical solution of a transmission problem with prefractal interface, Ph.D. thesis, Mathematical Sciences Department, WPI (2007).